Polyhedron 42 (2012) 128–134

Contents lists available at SciVerse ScienceDirect

Polyhedron

journal homepage: www.elsevier.com/locate/poly

Dianion N^1,N^4-bis(salicylidene)-*S*-allyl-thiosemicarbazide complexes: Synthesis, structure, spectroscopy and thermal behavior

Mehdi Ahmadi [a], Joel T. Mague [b], Alireza Akbari [a], Reza Takjoo [c,*]

[a] Department of Chemistry, Payame Noor University (PNU), 19395-4697 Tehran, Iran
[b] Department of Chemistry, Tulane University, New Orleans, LA 70118, USA
[c] Department of Chemistry, School of Sciences, Ferdowsi University of Mashhad, Mashhad 91775-1436, Iran

ARTICLE INFO

Article history:
Received 28 March 2012
Accepted 5 May 2012
Available online 14 May 2012

Keywords:
Isothiosemicarbazide
N_2O_2 donor
TGA
Spectroscopy
Crystal structures

ABSTRACT

The products with the general formulas VO(Salits) **1**, Mn(Salits)Br **2**, Fe(Salits)Cl **3** and UO_2(Salits)(MeOH) **4** (Salits = N^1,N^4-bis(salicylidene)-*S*-allyl-thiosemicarbazide) are prepared by the reaction of salicylaldehyde-*S*-allyl-thiosemicarbazone (H_2L) and salicylaldehyde with $VOSO_4{\cdot}3H_2O$, $Mn(CH_3COO)_2{\cdot}4H_2O$, $FeCl_3{\cdot}6H_2O$ and $UO_2(CH_3COO)_2{\cdot}2H_2O$, respectively. Complexes **1**–**4** were characterized by elemental analysis, spectroscopic (FT-IR and UV–Vis) and TGA techniques. Crystal and molecular structures of the complexes were determined by single crystal X-ray diffraction. The results revealed that the complexes **1**, **2** and **3** contain a dideprotonated tetradentate form of Salits coordinated via N_2O_2 donors along with oxido, bromido or chlorido ligands, respectively, and they have distorted square pyramidal geometries. However, the complex **4** adopts a severely distorted pentagonal bipyramidal geometry consisting of N_2O_2 coordination of Salits, a methanol ligand and two oxygens of the uranyl moiety. TG analysis showed that complex **3** is more stable than the others.

1. Introduction

The tetradentate ligands with the N_2O_2 donor set and their metal complexes are of great importance in chemistry as they provide synthetic models for the metal-containing sites in metallo-proteins and metallo-enzymes and extensive catalytic and bioactive applications. The prototype of this group is Salen. Since the first synthesis of Salen compounds in 1869 [1], many theoretical and empirical studies on these compounds and their complexes have been done [2], and a wide range of their properties such as bioactivity [3], catalytic [4,5], phosphorescence and electroluminescence [6] have been investigated.

In contrast to Salen-like compounds, bis(salicylidene)isothiosemicarbazides (Scheme 1a) with a similar structure have been less studied.

These compounds were synthesized and characterized for the first time in 1971 [7]. Since that time, few studies have been done on them and only a few crystal structures of their complexes have been reported, all of which are complexes of the *S*-methyl and *S*-propyl analogues [8–14].

In this paper, such compounds are briefly called "Salits". They have structures similar to that of the Salen-type ligands and are expected to manifest similar properties although the presence of a sulfur atom in the main skeleton may change some of their properties such as the biological [15], catalytic [16,17] or solubility. Considering the presence of the *N*-salicylideneaniline fragment in the $Salits_s$ ligand, one can expect photochromism for these materials as well [18]. The "Half-Salits" ligands (Scheme 1b) have been studied extensively; however, very few Salits compounds (Scheme 1a) have been prepared and no studies of their properties and applications have been done so far. Therefore, studies on the synthesis, characterization, structure and properties of the Salits compounds can be very important in inorganic chemistry and materials science.

In this study, four new complexes, N^1,N^4-bis(salicylidene)-*S*-allyl-isothiosemicarbazidato)oxidovanadium(IV) **1**, bromido(N^1,N^4-bis(salicylidene)-*S*-allyl-isothiosemicarbazidato)manganese(III) **2**, chlorido(N^1,N^4-bis(salicylidene)-*S*-allyl-isothiosemicarbazidato) iron(III) **3** and methanol(N^1,N^4-bis(salicylidene)-*S*-allyl-isothiosemicarbazidato)dioxidouranium(VI) **4** have been synthesized and characterized by spectroscopic and TG analysis and their structures have been determined by X-ray crystallography.

2. Experimental

2.1. Materials and instrumentation

All chemicals and solvents were of analytical reagent grade and were used without any further purification.

* Corresponding author. Tel./fax: +98 511 8975457.
E-mail address: rezatakjoo@yahoo.com (R. Takjoo).

0277-5387/$ - see front matter © 2012 Elsevier Ltd. All rights reserved.
http://dx.doi.org/10.1016/j.poly.2012.05.004

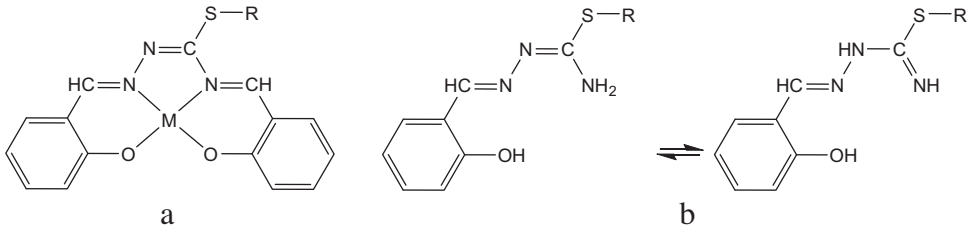

Scheme 1. (a) The general structure of Salits$_s$ and (b) the tautomery in half-Salits$_s$ (H_2L).

Microanalyses for C, H, N and S were performed on a Thermo Finnigan Flash Elemental Analyzer 1112EA. Molar conductances of ca. 10^{-3} M solutions of the complexes in methanol were measured by means of a Metrohm 712 Conductometer. IR spectra were recorded on a FT-IR 8400-SHIMADZU spectrophotometer with samples prepared as KBr (400–4000 cm^{-1}) pellets. The electronic spectra of the compounds were run in methanol solutions on a SHIMADZU model 2550 UV–Vis spectrophotometer in the range of 220–900 nm. The TGA diagrams were recorded in a TGA-50 SHIMADZU instrument at a heating rate of 10 °C/min in a air atmosphere over the temperature range of 20–850 °C. Diffraction data were measured using a Bruker Smart APEX CCD diffractometer.

2.2. Preparation of salicylaldehyde S-allyl-isothiosemicarbazone hydrobromide (H_2L)

A solution of thiosemicarbazide (0.46 g, 0.50 mmol) in ethanol (10 ml) was treated with allyl bromide (0.60 ml, 0.55 mmol) and was refluxed for 1 h. An ethanolic solution (5 ml) of salicylaldehyde (0.61 g, 0.50 mmol) was then added and the reflux continued for extra 2 h. The resulted yellow precipitate was filtered off, washed with cold ethanol and dried in vacuum over silica gel.

Yellow solid. Yield: 1.365 g (83%). Mp = 185 °C. UV–Vis (methanol): λ_{max} (ε_{max}) 228, 292, 302, 332 and 402 nm (27450, 33200, 33950, 38300 and 1150 M^{-1} cm^{-1}). IR (KBr, cm^{-1}) 3240(w), 3100(w), 1628(s), 1581(w), 1443(m), 1413(w), 1335(m), 1257(m), 1142(m), 933(w), 764(m), 625(m), 544(w), 478(w). *Anal.* Calc. for $C_{11}H_{14}BrN_3OS$ (316.22 g mol^{-1}): C, 41.78; H, 4.46; N, 13.29; S, 10.14. Found: C, 41.86; H, 4.55; N, 13.18; S, 9.98%.

2.3. General method for preparation of the complexes

A mixture of H_2L (0.5 mmol), the appropriate metal salt ($VOSO_4{\cdot}3H_2O$, $Mn(CH_3COO)_2{\cdot}4H_2O$, $FeCl_3{\cdot}6H_2O$ or $UO_2(CH_3COO)_2{\cdot}2H_2O$) (0.5 mmol) and salicylaldehyde (0.6 mmol) in ethanol (5 ml) was heated at 100 °C for 2 h. The product crystallized after several days at room temperature. (Hint: methanol was used as a solvent for uranium-complex preparation.)

2.3.1. N^1,N^4-bis(salicylidene)-S-allyl- isothiosemicarbazidato) oxidovanadium(IV) (1)

Slat, yellow. Mp = 222 °C. Molar conductivity (1×10^{-3} mol L^{-1}; DMF): 10 Ω^{-1} cm^2 mol^{-1}. UV–Vis (methanol): λ_{max} (ε_{max}) 228sh, 314, 340sh, 416 and 650 nm (72550, 31850, 24550, 13500 and 171 M^{-1} cm^{-1}). IR (KBr, cm^{-1}) 1605(s), 1575(s), 1535(s), 1512(m), 1427(m), 1373(m), 1296(m), 1203(w), 1142(mb), 980(s), 918(w), 802(w), 764(m), 602(w), 494(w). *Anal.* Calc. for $C_{18}H_{15}N_3O_3SV$ (404.34 g mol^{-1}): C, 53.47; H, 3.74; N, 10.39; S, 7.93. Found: C, 52.48; H, 3.69; N, 10.25; S, 7.79%.

2.3.2. Bromido(N1,N4-bis(salicylidene)-S-allyl-isothiosemicarbazidato)manganese(III)" (**2**)

Tablet, brown. Mp >300 °C. Molar conductivity (1×10^{-3} mol L^{-1}; DMF): 110 Ω^{-1} cm^2 mol^{-1}. UV–Vis (methanol): λ_{max} (ε_{max}) 246, 334, 436 and 478sh nm (39100, 29900, 9900 and 7450 M^{-1} cm^{-1}). IR (KBr, cm^{-1}) 1603(s), 1574(s), 1527(m), 1506(m), 1427(w), 1373(w), 1288(m), 1203(w), 1141(m), 1119(m), 1026(w), 918(w), 810(w), 764(w), 671(w), 609(w), 501(vw). *Anal.* Calc. for $C_{18}H_{15}BrMnN_3O_2S$ (472.24 g mol^{-1}): C, 45.78; H, 3.20; N, 8.90; S, 6.79. Found: C, 45.36; H, 3.19; N, 8.76; S, 6.85%.

2.3.3. Chlorido(N^1,N^4-bis(salicylidene)-S-allyl-isothiosemicarbazidato) iron(III) (3)

Plate, brown. Mp = 223 °C. Molar conductivity (1×10^{-3} mol L^{-1}; DMF): 27 Ω^{-1} cm^2 mol^{-1}. UV–Vis (methanol): λ_{max} (ε_{max}) 238, 278sh, 306, 372, 430 and 608 nm (27650, 22500, 31000, 12550 and 1250 M^{-1} cm^{-1}). IR (KBr, cm^{-1}) 1606(s), 1574(s), 1527(m), 1506(m), 1427(w), 1373(w), 1296(m), 1142(m), 1026(w), 810(w), 764(w), 671(w), 602(w), 510(vw). *Anal.* Calc. for $C_{18}H_{15}ClFeN_3O_2S$ (428.69 g mol^{-1}): C, 50.43; H, 3.53; N, 9.80; S, 7.48. Found: C, 49.65; H, 3.49; N, 9.69; S, 7.34%.

2.3.4. Methanol(N^1,N^4-bis(salicylidene)-S-(allyl)-isothiosemicarbazidato)dioxidouranium(VI) (**4**)

Block, red. Mp = 190 °C. Molar conductivity (1×10^{-3} mol L^{-1}; DMF): 4 Ω^{-1} cm^2 mol^{-1}. UV–Vis (methanol): λ_{max} (ε_{max}) 238sh, 280, 326, 338 and 446 nm (16200, 15850, 13200, 12500 and 2500 M^{-1} cm^{-1}). IR (KBr, cm^{-1}) 1605(s), 1573(s), 1527(s), 1465(m), 1427(m), 1388(m), 1288(m), 1203(w), 1142(m), 1011(w), 910(w), 756(w), 671(m), 586(w), 440(w). *Anal.* Calc. for $C_{19}H_{19}N_3O_5SU$ (639.47 g mol^{-1}): C, 35.69; H, 2.99; N, 6.57; S, 5.01. Found: C, 35.36; H, 2.93; N, 6.56; S, 4.97%.

2.4. Crystallography

The crystals of **1**–**4** were mounted on a Cryoloop™ with a film of Paratone™ oil and transferred to the goniometer head attached to the Bruker-AXS Smart APEX diffractometer where they were cooled to 100 K with a nitrogen cold-stream. Complete spheres of data were collected under control of APEX2/BIS [19] following which ca. 1500–2200 reflections having $I/\sigma(I) \geq 15$ were used to determine approximate unit cell parameters. From these results, **1** and **4** were found to be single crystals, **2** was triclinic and consisted of one major and 2–3 minor domains (determined with CELL-NOW) [20] and **3** was a 2-component triclinic crystal with the two domains rotated 10.6° about the axis (0.65, 0.43, 1.00). Integration of the raw intensities, application of Lorentz and polarization corrections and global refinement of unit cell parameters (using 7138–9973 reflections) was performed with SAINT [21] using 1-component control files for **1** and **4**, the control file for the major component of **2** as generated by CELL-NOW and the 2-component control file for **3** as generated by CELL-NOW. Absorption corrections (GAUSSIAN integration based on indexing of the crystal faces for **1** and use of equivalent reflections from different regions of reciprocal space for the others) were applied with SADABS [22] for **1**, **2** and **4** and with TWINABS [23] for **3**. Heavy atom positions were determined from Patterson functions (SHELXS) [24] and the remainder of

Table 1
Crystal data and structure refinement.

Complex	**1**	**2**	**3**	**4**
Formula	$C_{18}H_{15}N_3O_3SV$	$C_{18}H_{15}BrMnN_3O_2S$	$C_{18}H_{15}ClFeN_3O_2S$	$C_{19}H_{18}N_3O_5SU$
Formula weight	404.33	472.24	428.69	638.45
T (K)	100(2)	100(2)	100(2)	100(2)
λ (Å)	0.71073	0.71073	0.71073	0.71073
Crystal system	triclinic	triclinic	triclinic	monoclinic
Space group	$P\bar{1}$	$P\bar{1}$	$P\bar{1}$	$C2/c$
Unit cell dimensions				
a (Å)	7.0279(13)	7.2641(15)	7.213(2)	40.399(7)
b (Å)	9.6498(18)	9.755(2)	9.701(3)	11.389(2)
c (Å)	13.257(3)	13.527(3)	13.571(5)	19.186(4)
α (°)	72.974(2)	71.905(3)	72.477(3)	
β (°)	82.838(2)	80.600(3)	81.568(5)	108.209(2).
γ (°)	80.277(3)	76.065(3)	77.517(3)	
V (Å^3)	844.6(3)	880.2(3)	880.8(5)	8386(3)
Z	2	2	2	16
D_{calc} (Mg/m^3)	1.590	1.782	1.616	2.023
Absorption coefficient (mm^{-1})	0.735	3.157	1.144	7.877
F(000)	414	472	438	4816
Crystal size (mm)	0.27 × 0.07 × 0.04	0.12 × 0.08 × 0.05	0.22 × 0.10 × 0.02	0.22 × 0.18 × 0.12
θ range for data collection (°)	2.23–29.03	2.24–29.05	1.58–28.34	1.87–28.34
Index ranges	$-9 \le h \le 9$, $-11 \le k \le 12$, $-17 \le l \le 17$	$-9 \le h \le 9$, $-13 \le k \le 13$, $-18 \le l \le 18$	$-9 \le h \le 9$, $-11 \le k \le 12$, $-18 \le l \le 18$	$-53 \le h \le 53$, $-15 \le k \le 15$, $-25 \le l \le 25$
Reflections collected	14661	15516	14884	71144
Independent reflections	4209 [R_{int} = 0.0436]	4411 [R_{int} = 0.0317]	3930 [R_{int} = 0.0353]	10271 [R_{int} = 0.0652]
Absorption correction	semi-empirical from equivalents	semi-empirical from equivalents	semi-empirical from equivalents	numerical
Maximum and minimum transmission	0.9705 and 0.7519	0.8581 and 0.6933	0.9775 and 0.7844	0.4466 and 0.2434
Data/restraints/parameters	4209/7/254	4411/3/244	3930/8/254	10271/138/511
Goodness-of-fit (GOF) on F^2	1.071	1.064	1.056	1.022
Final R indices [$I > 2\sigma(I)$]	R_1 = 0.0439, wR_2 = 0.1025	R_1 = 0.0322, wR_2 = 0.0809	R_1 = 0.0583, wR_2 = 0.1513	R_1 = 0.0349, wR_2 = 0.0756
R indices (all data)	R_1 = 0.0547, wR_2 = 0.1081	R_1 = 0.0377, wR_2 = 0.0833	R_1 = 0.0695, wR_2 = 0.1588	R_1 = 0.0485, wR_2 = 0.0809
Largest diff. peak and hole (e Å^{-3})	0.433 and −0.621	0.926 and −0.532	1.256 and −1.156	1.940 and −1.680

the structures developed by the repeated cycles of full-matrix, least-squares refinement followed by the calculation of a difference Fourier synthesis (SHELXL) [24]. In the case of **4**, there are two crystallographically independent molecules in the asymmetric unit while for the others the asymmetric unit consists of a single molecule. In all four complexes, the bis(Schiff base) ligand is disordered end-to-end in the ratios 68:32 (**1**), 57:43 (**2**), 56:44 (**3**) and 75:25 (**4**, each independent molecule). Because the ligand, with the exception of the {N=C–S–CH_2–CH=CH_2} portion, is symmetrical, there is no significant effect of the disorder on the extremities but there are two separate locations of the S-allyl side-chain. This disorder was modeled by refining two locations of the full {N=C–S–CH_2–CH=CH_2} portion with restraints to make both components of the disorder have approximately the same geometry and have the sum of the occupancies of the two components be 1.0. All H-atoms were included as riding contributions in idealized positions with isotropic displacement parameters. For **3**, trial refinements with the full 2-component reflection file and with the 1-component file for the major component extracted from the full data set with TWINABS showed that the latter refinement was superior. Calculations not noted above were performed with SHELXTL [25]. The crystal data and structural refinement parameters for complexes are listed in Table 1.

3. Results and discussion

The complexes **1**–**4** were prepared via a straightforward template method which involves the direct reactions of H_2L, salicylaldehyde and the appropriate metal salt in a 1:1:1 M ratio in ethanol or methanol as solvent. All the obtained structures were predictable except for that of **2** where the bromide ion of H_2L became coordinated to Mn, resulting in a metal oxidation number of +3.

The complexes **1** and **2** are the first examples of the family of vanadium and manganese "Salits" complexes with the square pyramidal structure for which the structures have been determined by X-ray crystallography (for Salits complexes as a whole, **2** is the second complex of manganese to be structurally characterized) so far.

All the complexes are soluble in common organic solvents such as DMF, DMSO, chloroform, alcohols and are insoluble in water. The molar conductance values show that **1**, **3** and **4** behave essentially as non-electrolytes in methanol, while **2** is a 1:1 electrolyte which can be explained by the following reaction. Such a phenomenon has been reported previously [26].

$$[Mn(Salits)Br] + MeOH \rightarrow [Mn(Salits)MeOH]^+ + Br^-$$

3.1. IR

The IR spectra of the complexes exhibit several prominent bands in the 500–4000 cm^{-1} region. Because the preparation of the ligand and complexes is done in one step, we cannot make a comparison between the IR spectra of the complexes and the corresponding ligand although the IR data for the H_2L precursor can provide a starting point for the interpretation of the spectra of the complexes.

The infrared absorptions at 3240 and 3100 cm^{-1}, which are attributed to the OH and NH_2 functional groups and are seen in salicylaldehyde and H_2L, are absent in the spectra of the complexes. The deletion of υ(OH) and υ(NH_2) peaks and the formation of C=N bonds demonstrate the condensation reaction of aldehyde and thioamide in the presence of metal ion. Using the υ(C=N) absorption band in H_2L as a guide, we assign the two strong bands at 1606–1603 and 1575–1573 cm^{-1} to υ(C=N) [27,28]. In addition,

the medium intensity absorptions in the 1296–1288 cm^{-1} region were assigned to the υ(Ar–O) vibration mode [18,29] and the intense band in the region 1535–1527 cm^{-1} is assigned to the C=C vibration [30]. The 1427 cm^{-1} band is assigned to the NCS stretching vibration [31], while the $(U{=}O)_{asy}$ and V=O frequencies appear at 910 and 980 cm^{-1}, respectively [32,33].

3.2. UV–Vis absorption spectra of complexes

All the absorption spectra of the complexes in diluted methanol solutions are listed in the experimental section. In the high-energy region, below 300 nm, two absorption bands were detected which are related to $\pi \rightarrow \pi^*$ transitions of the phenyl rings [34]. The electronic spectra of complexes show two intense bands which are attributable to $\pi \rightarrow \pi^*$ and $n \rightarrow \pi^*$ transitions of the azomethine chromophore below 400 nm [28,35], while phenoxide-to-metal ion charge-transfer transitions appear in the region 416–478 nm. Complexes **1** and **3** show d–d transitions at 650 and 608 nm, respectively, but the d–d transitions were not observed for the others because they are covered by charge-transfer and intraligand transition bands.

3.3. Thermogravimetric analysis

Thermogravimetric analysis (TGA) has been done to investigate the physical behavior of the complexes and their thermograms are presented in Supplementary material.

In complex **1** the TGA curve shows an initial 9.87% (Calc. 10.16%) weight loss, which is in a good agreement with the removal of an allyl group, followed by the second loss in the 315–427 °C range in which the sulfur atom of the ligand is separated and results in 8.48% (Calc. 8.82%) decrease in weight. Eventually, the remainder is decomposed to stable VO_2 residue with a concomitant 76.59% (Calc. 76.57) weight loss relative to the initial material.

Complex **2** decomposes in three endothermic steps which can be seen on the DTA curve (20–244, 481–637 and 709–787 °C). In the first step, it loses 8.90% (Calc. 8.77%) of its weight with the removal of an allyl group. In the two other steps the bromide is eliminated at 481–637 °C with a weight loss of 18.61% (Calc. 18.55%). Major mass losses occur at 709–787 °C attributed to decomposition to Mn_2O_3 with a weight loss of 81.25% (Calc. 83.28%) relative to complex **2**.

For the Fe complex, the TGA curve shows that the thermal decomposition of the complex occurs within the temperature ranges of 243–277 and 427–530 °C. The first step of gradual thermal changes on the DTG curve is attributed to the removal of allyl sulfide with a weight loss of 17.27% (Calc. 17.06%). The last DTG peak, having a maximum at 488.8 °C, demonstrates a large weight loss of about 61.33% (Calc. 61.9%) and it is due to rapid thermal decomposition of the remainder to Fe_3O_4.

The TG/DTG curves of compound **4** indicates four thermal decomposition steps at 171–215, 315–350, 470–542 and 646–702 °C, respectively. The TG/DTG curves of compound **4** reveal a prominent stability up to its melting point at 191 °C. At this point, 171–215 °C, the methanol molecules, and therefore, a 5% (Calc. 5.02%) reduction in its weight can be seen. In the second step, over the 315–350 °C range (maximum 341 °C), the elimination of –CH=N–C–S-allyl takes place which is revealed by a 18.68% (Calc. 18.49%) weight loss. The –O–Ph–CH=N–N– fragment is rapidly removed in the third step, which is consistent with a 27.47% (Calc. 26.93%) decrease in weight at 470–542 °C. The last TGA peak, with its maximum at 686 °C is attributable to the presence of U_3O_8 residue [36].

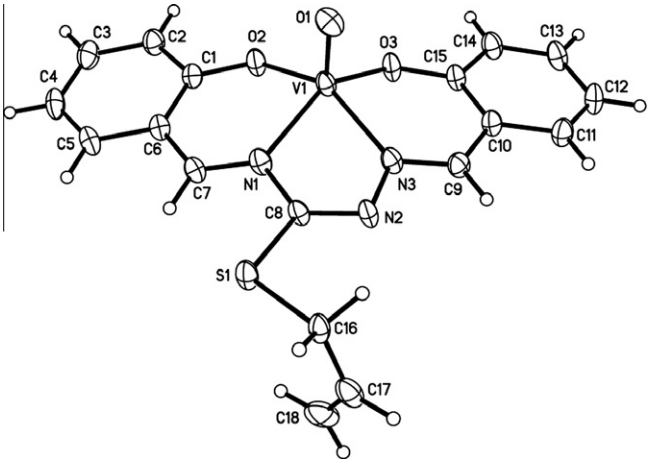

Fig. 1. Perspective view of **1**. Displacement ellipsoids are drawn at the 50% probability level and H-atoms are shown as spheres of arbitrary radius.

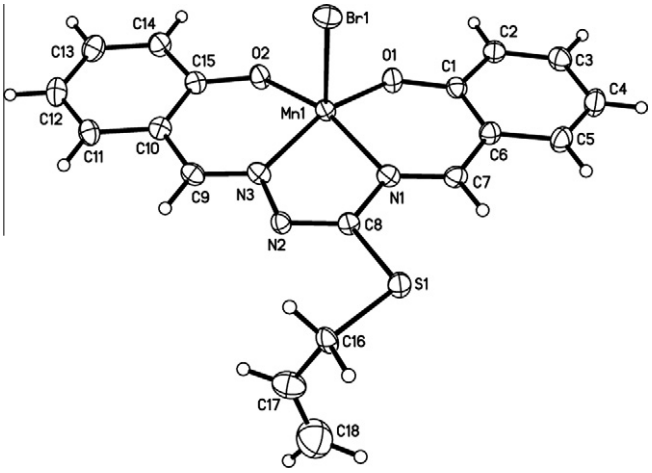

Fig. 2. Perspective view of **2**. Displacement ellipsoids are drawn at the 50% probability level and H-atoms are shown as spheres of arbitrary radius.

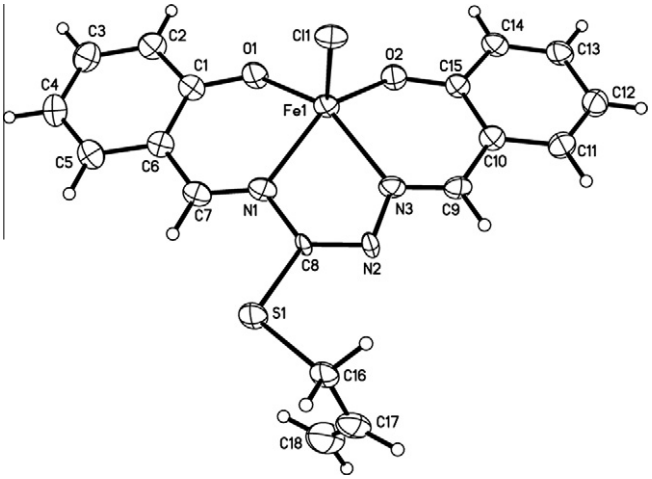

Fig. 3. Perspective view of **3**. Displacement ellipsoids are drawn at the 50% probability level and H-atoms are shown as spheres of arbitrary radius.

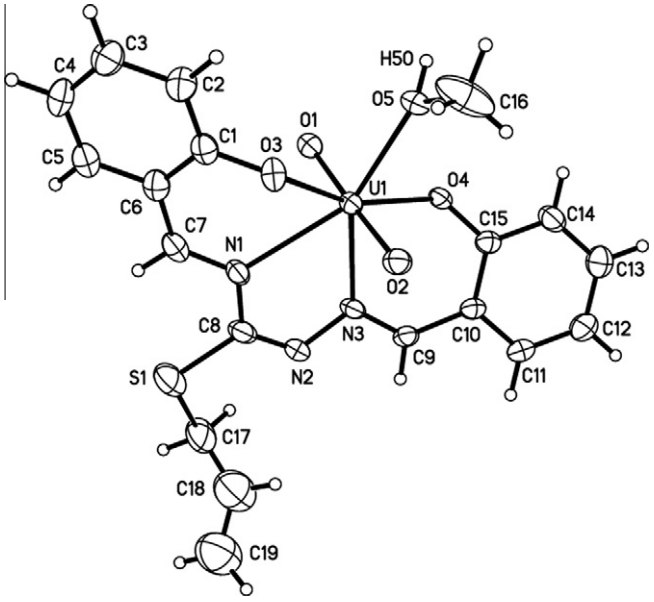

Fig. 4. Perspective view of molecule 1 for **4**. Displacement ellipsoids are drawn at the 50% probability level and H-atoms are shown as spheres of arbitrary radius.

Table 3
Bond lengths (Å) and angles (°) for **4**.

U(1)–O(1)	1.775(4)	U(2)–O(6)	1.774(4)
U(1)–O(2)	1.776(4)	U(2)–O(7)	1.776(4)
U(1)–O(3)	2.238(4)	U(2)–O(8)	2.230(4)
U(1)–O(4)	2.299(3)	U(2)–O(9)	2.296(4)
U(1)–O(5)	2.395(4)	U(2)–O(10)	2.403(3)
U(1)–N(3)	2.560(4)	U(2)–N(4)	2.555(5)
U(1)–N(1)	2.566(4)	U(2)–N(6)	2.574(4)
O(1)–U(1)–O(2)	177.58(16)	O(6)–U(2)–O(7)	178.89(17)
O(1)–U(1)–O(3)	91.50(15)	O(6)–U(2)–O(8)	88.70(18)
O(2)–U(1)–O(3)	88.82(16)	O(7)–U(2)–O(8)	90.62(16)
O(1)–U(1)–O(4)	85.84(15)	O(6)–U(2)–O(9)	94.94(17)
O(2)–U(1)–O(4)	93.07(15)	O(7)–U(2)–O(9)	85.40(16)
O(3)–U(1)–O(4)	160.99(13)	O(8)–U(2)–O(9)	159.83(14)
O(1)–U(1)–O(5)	88.13(15)	O(6)–U(2)–O(10)	89.43(15)
O(2)–U(1)–O(5)	89.56(15)	O(7)–U(2)–O(10)	89.60(15)
O(3)–U(1)–O(5)	81.24(13)	O(8)–U(2)–O(10)	80.52(13)
O(4)–U(1)–O(5)	79.85(13)	O(9)–U(2)–O(10)	79.69(13)
O(1)–U(1)–N(3)	99.85(15)	O(6)–U(2)–N(4)	98.25(17)
O(2)–U(1)–N(3)	81.78(15)	O(7)–U(2)–N(4)	82.34(16)
O(3)–U(1)–N(3)	128.88(14)	O(8)–U(2)–N(4)	70.68(15)
O(4)–U(1)–N(3)	70.05(13)	O(9)–U(2)–N(4)	128.04(15)
O(5)–U(1)–N(3)	148.06(13)	O(10)–U(2)–N(4)	149.90(15)
O(1)–U(1)–N(1)	83.10(15)	O(6)–U(2)–N(6)	82.81(16)
O(2)–U(1)–N(1)	99.26(15)	O(7)–U(2)–N(6)	98.30(15)
O(3)–U(1)–N(1)	70.41(14)	O(8)–U(2)–N(6)	130.20(15)
O(4)–U(1)–N(1)	127.70(13)	O(9)–U(2)–N(6)	69.97(15)
O(5)–U(1)–N(1)	150.01(14)	O(10)–U(2)–N(6)	147.79(15)
N(3)–U(1)–N(1)	61.94(14)	N(4)–U(2)–N(6)	62.30(17)

3.4. X-ray crystal structures

Perspective views of complexes **1**–**4** are presented in Figs. 1–4, respectively, while relevant bond distances and interbond angles for **1**–**3** are listed in Table 2 and those for **4** are given in Table 3. Primarily because of the S-allyl side-chain, the ligand is unsymmetrical overall, but since the backbone structure and particularly the four donor atoms are essentially symmetrical, there is no preferred orientation of the ligand with respect to the metal as the template reaction forms it. Consequently, with the presence of the fifth ligand in the final complex in **1**–**3** to provide a "top/bottom" (or "left/right") reference point, two isomers are possible (Scheme 2). It appears from the X-ray results that both isomers have been formed and have co-crystallized since the N=C–S-allyl portion is disordered over two sites in varying amounts in all three complexes. In the case of **4** two co-crystallized isomers must still be present from the observed positional disorder in the S-allyl group. Similar results have previously been seen with related complexes [8,14]. Only the major isomer is shown in Figs. 1–4. The structures of **1**–**3** are all very similar with the coordination sphere being a slightly distorted square pyramid having the tetradentate ligand in the basal plane. The ligand geometries vary relatively little among **1**–**3** as well among several close analogues (Table 4). The principal distortions of the coordination sphere from ideal square

Table 2
Bond lengths (Å) and angles (°) for **1**–**3**.

1		**2**		**3**	
V(1)–O(3)	1.9265(16)	Mn(1)–O(2)	1.8690(16)	Fe(1)–O(2)	1.886(3)
V(1)–O(2)	1.9404(16)	Mn(1)–O(1)	1.8773(16)	Fe(1)–O(1)	1.889(3)
V(1)–N(3)	2.0519(19)	Mn(1)–N(3)	1.9735(19)	Fe(1)–N(3)	2.091(3)
V(1)–N(1)	2.0625(19)	Mn(1)–N(1)	1.9810(19)	Fe(1)–N(1)	2.106(3)
V(1)–O(1)	1.5968(18)	Mn(1)–Br(1)	2.5324(6)	Fe(1)–Cl(1)	2.2482(11)
C(1)–O(2)	1.315(3)	C(1)–O(1)	1.321(3)	C(1)–O(1)	1.312(4)
C(1)–C(6)	1.427(3)	C(1)–C(6)	1.427(3)	C(1)–C(6)	1.429(5)
C(6)–C(7)	1.419(3)	C(6)–C(7)	1.419(3)	C(6)–C(7)	1.428(5)
C(7)–N(1)	1.305(3)	C(7)–N(1)	1.314(3)	C(7)–N(1)	1.305(5)
N(1)–C(8)	1.459(5)	N(1)–C(8)	1.467(8)	N(1)–C(8)	1.473(12)
C(8)–N(2)	1.290(4)	C(8)–N(2)	1.280(6)	C(8)–N(2)	1.274(10)
N(2)–N(3)	1.371(5)	N(2)–N(3)	1.357(7)	N(2)–N(3)	1.354(9)
N(3)–C(9)	1.310(3)	N(3)–C(9)	1.301(3)	N(3)–C(9)	1.298(5)
C(9)–C(10)	1.420(3)	C(9)–C(10)	1.435(3)	N(3)–C(9)	1.429(5)
C(10)–C(15)	1.432(3)	C(10)–C(15)	1.424(3)	C(10)–C(15)	1.430(5)
O(3)–V(1)–O(2)	89.83(7)	O(2)–Mn(1)–O(1)	92.82(7)	O(2)–Fe(1)–O(1)	96.78(11)
O(3)–V(1)–N(3)	86.95(7)	O(2)–Mn(1)–N(3)	91.30(7)	O(2)–Fe(1)–N(3)	86.60(11)
O(2)–V(1)–N(3)	145.70(8)	O(1)–Mn(1)–N(3)	160.57(8)	O(1)–Fe(1)–N(3)	148.53(12)
O(3)–V(1)–N(1)	141.52(8)	O(2)–Mn(1)–N(1)	161.08(8)	O(2)–Fe(1)–N(1)	145.33(12)
O(2)–V(1)–N(1)	87.10(7)	O(1)–Mn(1)–N(1)	91.65(8)	O(1)–Fe(1)–N(1)	86.61(11)
N(3)–V(1)–N(1)	74.80(8)	N(3)–Mn(1)–N(1)	78.73(8)	N(3)–Fe(1)–N(1)	73.79(12)
O(1)–V(1)–O(3)	109.76(8)	O(2)–Mn(1)–Br(1)	101.27(6)	O(2)–Fe(1)–Cl(1)	107.43(9)
O(1)–V(1)–O(2)	109.20(9)	O(1)–Mn(1)–Br(1)	101.16(6)	O(1)–Fe(1)–Cl(1)	107.34(9)
O(1)–V(1)–N(3)	104.00(9)	N(3)–Mn(1)–Br(1)	96.53(6)	N(3)–Fe(1)–Cl(1)	101.33(9)
O(1)–V(1)–N(1)	107.43(8)	N(1)–Mn(1)–Br(1)	95.97(6)	N(1)–Fe(1)–Cl(1)	104.33(8)

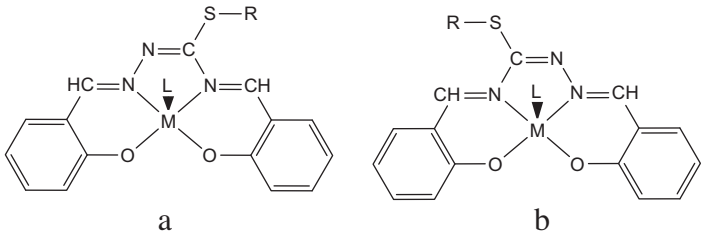

Scheme 2. The two co-crystallized isomers of **1**–**3**.

Table 4
Comparison of Chelated ligand geometries (Å).[a]

	a	*b*	*c*	*d*	*e*	*f*	*g*	*h*	*i*	*j*	*k*	*l*	*m*
1	1.9404(16)	1.315(3)	1.419(3)	1.305(3)	2.0625(19)	1.459(5)	1.290(4)	1.371(5)	1.310(3)	1.420(3)	1.314(3)	1.9265(16)	2.0519(18)
2	1.8690(16)	1.321(3)	1.419(3)	1.314(3)	1.9737(19)	1.400(3)	1.315(4)	1.403(3)	1.300(3)	1.435(3)	1.320(3)	1.8773(16)	1.9806(19)
2′[b]	1.867(5)	1.318[b]	1.426[b]	1.315[b]	1.995(7)	1.392[b]	1.329[b]	1.403[b]	1.308[b]	1.428[b]	1.327[b]	1.893(6)	1.983(7)
3	1.889(3)	1.312(4)	1.428(5)	1.305(5)	2.106(3)	1.473(12)	1.27(1)	1.354(9)	1.298(5)	1.429(5)	1.311(4)	1.886(3)	2.091(3)
3′[c]	1.894(4)	1.31(1)	1.41(1)	1.31(1)	2.101(4)	1.40(1)	1.30(1)	1.40(1)	1.30(1)	1.43(1)	1.34(1)	1.875(4)	2.084(5)
3″[d]	1.905(4)	1.308(7)	1.416(9)	1.299(8)	2.106(5)	1.386(7)	1.314(8)	1.393(7)	1.301(8)	1.408(9)	1.319(7)	1.922(4)	2.101(5)
	1.903(4)	1.316(7)	1.409(9)	1.300(8)	2.103(5)	1.394(7)	1.300(8)	1.407(7)	1.317(8)	1.429(9)	1.317(7)	1.919(4)	2.097(5)
4	2.238(4)	1.344(4)	1.447(6)	1.302(7)	2.566(4)	1.410(12)	1.28(1)	1.402(9)	1.297(7)	1.461(6)	1.344(4)	2.299(3)	2.560(4)
	2.230(4)	1.335(5)	1.430(7)	1.301(8)	2.555(5)	1.499(9)	1.26(1)	1.338(8)	1.302(8)	1.436(8)	1.345(5)	2.296(4)	2.574(4)
4′	2.278(4)[e]	1.322(7)	1.431(9)	1.312(8)	2.575(5)	1.395(8)	1.277(9)	1.427(8)	1.292(8)	1.434(9)	1.305(7)	2.251(4)	2.548(5)
	2.263(3)[f]	1.297(6)	1.438(8)	1.287(7)	2.596(4)	1.415(7)	1272(7)	1.403(6)	1.294(6)	1.429(8)	1.337(5)	2.274(3)	2.549(4)

[a] See Fig. 5 for key to column headings.
[b] CCDC entry FEBCEU (Ref. [12]), M = MnCl(MeOH), R = Me, su's on light atom distances = 0.012.
[c] CCDC entry BOZCEY (Ref. [8]), M = FeCl, R = Me.
[d] CCDC entry CAWCIM (Ref. [9]), M = OFe(L_4), R = Me.
[e] CCDC entry EKEWUN (Ref. [13]), M = UO_2(*n*-nonylOH), R = *n*-Pr, triclinic form.
[f] CCDC entry EKEXAU (Ref. [13]), M = UO_2(*n*-nonylOH), R = *n*-Pr, monoclinic form.

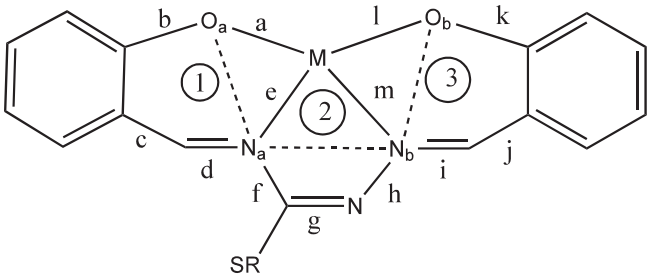

Fig. 5. Schematic of **1**–**3** as a key to the quantities in Tables 4 and 5.

pyramidal geometry are the small N1–M–N3 (M = V, Mn, Fe) angle resulted from geometric constraints of the ligand backbone and the displacement of the metal from the basal plane towards the axial ligand. The three chelate rings are not coplanar with the metal but each of the rings is folded about a line joining its two donor atoms as depicted by the dashed lines in Fig. 5. These fold angles in **1**–**3** together with the angles between the mean planes of the phenyl rings and the displacement of the metal from the basal plane are presented in Table 5 with corresponding data for several related complexes. In the 5-coordinate complexes, there is a rough correlation between both the extent of displacement of the metal from the N_2O_2 plane and the folding of the chelate rings and the length of the bond to the axial ligand with the displacement in the order X = O > Cl > Br. Addition of a sixth ligand to the metal substantially reduces the displacement and folding distortions as the bonding to the metal in the axial directions becomes more equalized (e.g. chlorido(methanol)(*S*-methyl-N^1,N^4-bis(salicylidene)isothiosemicarbazidato)manganese(III) [12] (Table 5) and thiocyanato(pyridine)(*S*-*methyl*-N^1,N^4-bis(salicylidene)isothiosemicarbazidato)iron(III) [11] (no distortion)).

Table 5
Conformational angles (°) for **1**–**3**.[a]

	Fold of ring 1along $O_a\cdots N_a$	Fold of ring 2along $N_a\cdots N_b$	Fold of ring 3along $O_b\cdots N_b$	Angle between mean planes of phenyl rings	Distance of metal from N_2O_2 plane (Å)
1	12.83(5)	17.5(2)	19.3(1)	18.7(1)	0.606(1)
2	11.3(4)	10.1(2)	9.47(9)	5.0(1)	0.297(1)
2′[b]	<1	6.3	<1	10.7	0.15
3	12.4(1)	15.5(5)	18.0(2)	12.9(2)	0.524(2)
3′[c]	17.8	14.7	18.7	4.0	0.53
3″[d]	15.8	17.2	24.7	9.9	0.61
	19.6	18.3	18.7	7.3	0.61

[a] See Fig. 5 for key to column headings.
[b] CCDC entry FEBCEU (Ref. [12]), M = MnCl(MeOH), R = Me.
[c] CCDC entry BOZCEY (Ref. [8]), M = FeCl, R = Me.
[d] CCDC entry CAWCIM (Ref. [9]), M = OFe(L_4), R = Me (su's unavailable for these values).

There are two independent molecules of **4** in the asymmetric unit and these primarily differ in the orientation of the allyl group with respect to the ligand backbone. As is evident from Fig. 4, the uranium is 7-coordinate but the geometry of the coordination sphere departs markedly from the expected pentagonal bipyramid.

If we take the plane defined by U1, O5, N1 and N3 as the "equatorial" plane, the axis of the nearly linear O1–U1–O2 unitis markedly inclined to it as depicted in Fig. 6. Thus the dihedral angle between the mean planes defined by U1, O5, N1 and N3 and by U1, O3, O4 and O5 is 19.4(2)° and the corresponding angle in molecule 2 is 18.3(2)°. The phenolic portions of the ligand adopt a propeller-like conformation with dihedral angles of 35.8(2)° and 37.6(3)°, respectively, for molecules 1 and 2. Similar distortions are seen in uranyl complexes of the *S*-methyl analogue of the li-

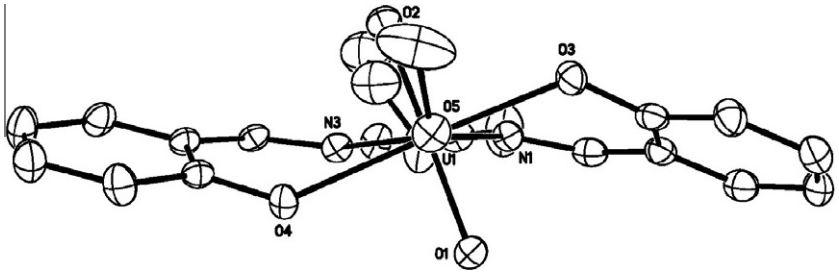

Fig. 6. View of **4** with the U1, O5, N1, N3 plane horizontal and showing the twist of the coordination about uranium.

gand employed here as well as ones with the *S*-propyl side chain plus two chlorine substituents on one of the aromatic rings. These range from large (20.8°) to small (6.5°) dihedral angles between the phenyl rings [13,37]. The distortions are likely, in part, to accommodate larger radius of uranium as compared with the first row transition elements and the resulting longer metal–donor atom distances in **4** without putting significant strain on the backbone of the ligand. Molecule 1 (containing U1) forms pair-wise H-bonds with molecule 2 (containing U2) at $x, y-1, z$ (H5O···O9 (at $x, y-1, z$) = 1.71 Å, O5–H5O···O9 = 162°; O4···H10O (at $x, y-1, z$) = 1.77 Å, O4···H10O–O10 = 150° while molecule 2 forms the corresponding H-bonds with molecule 1 at $x, y+1, z$.

4. Conclusion

In this study, we presented the synthesis and characterization of four new complexes of the novel ligand N^1,N^4-bis(salicylidene)-*S*-allyl-thiosemicarbazone (Salits). The spectral and X-ray studies show that this ligand behaves as a dinegative tetradentate N_2O_2 chelate in the presence of metal ions. In **1**–**3**, a fifth coordination site is occupied by oxygen, bromide and chloride atoms, respectively. This results in a distorted square pyramidal geometry. For complex **4**, in addition to Salits, two oxygen atoms and a methanol molecule were coordinated to uranium(VI), giving rise to a considerably distorted pentagonal bipyramid geometry. The TG analyses of **1**–**4** show that they are decomposed at above ca. 190 °C, and finally give a metal oxide residue.

Acknowledgements

We would like to thank the Tulane University Chemistry Department for support of the Tulane Crystallography Laboratory; and the Ferdowsi University of Mashhad and Payame Noor University (PNU) for financial supports.

Appendix A. Supplementary data

CCDC 832353–832356 contain the supplementary crystallographic data for **1**–**4**. These data can be obtained free of charge via http://www.ccdc.cam.ac.uk/conts/retrieving.html, or from the Cambridge Crystallographic Data Centre, 12 Union Road, Cambridge CB2 1EZ, UK; fax: (+44) 1223-336-033; or e-mail: deposit@ccdc.cam.ac.uk. Supplementary data associated with this article can be found, in the online version, at http://dx.doi.org/10.1016/j.poly.2012.05.004. TGA and derivative of TGA curves of complexes are given as Supplementary publication.

References

[1] H. Schiff, Liebigs Ann. Chem. 150 (1869) 193.
[2] J. Costamagna, J. Vargas, R. Latorre, A. Alvarado, G. Mena, Coord. Chem. Rev. 119 (1992) 67.
[3] K.I. Ansari, J.D. Grant, S. Kasiri, G. Woldemariam, B. Shrestha, S.S. Mandal, J. Inorg. Biochem. 103 (2009) 818.
[4] S.M. Bruno, S.S. Balula, A.A. Valente, F.A. Almeida Paz, M. Pillinger, C. Sousa, J. Klinowski, C. Freire, P. Ribeiro-Claro, I.S. Gonçalves, J. Mol. Catal. A 270 (2007) 185.
[5] Y.N. Belokon, J. Fuentes, M. North, J.W. Steed, Tetrahedron 60 (2004) 3191.
[6] Ch.-M. Che, S.-Ch. Chan, H.-F. Xiang, M.C.W. Chan, Y. Liu, Y. Wang, Chem. Commun. (2004) 1484.
[7] N.V. Gerbeleu, M.D. Revenco, Russ. J. Inorg. Chem. 16 (1971) 1046.
[8] M.A. Yampol'skaya, S.G. Shova, N.V. Gerbeleu, V.K. Bel'skii, Yu.A. Simonov, Zh. Neorg. Khim. 27 (1982) 2551.
[9] M.A. Yampol'skaya, S.G. Shova, N.V. Gerbeleu, Yu.A. Simonov, V.K. Bel'skii, A.A. Dvorkin, Zh. Neorg. Khim. 28 (1983) 1744.
[10] T.I. Malinovskii, Yu.A. Simonov, M.A. Yampol'skaya, S.G. Shova, M.D. Revenko, V.G. Rusu, Acta Crystallogr., Sect. A 40 (1984) C310.
[11] Yu.A. Simonov, M.A. Yampol'skaya, S.G. Shova, V.K. Bel'skii, N.V. Gerbeleu, Dokl. Akad. Nauk SSSR 282 (1985) 895.
[12] M.D. Revenko, N.V. Gerbeleu, V.G. Rusu, S.G. Shova, Yu.A. Simonov, Zh. Neorg. Khim. 31 (1986) 1737.
[13] M. Şahin, A. Koca, N. Özdemir, M. Dinçer, O. Büyükgüngör, T. Bal-Demirci, B. Ülküseven, Dalton Trans. 39 (2010) 10228.
[14] V.M. Leovac, E.Z. Ivegeš, N. Galešić, D. Horvatić, Inorg. Chim. Acta 162 (1989) 277.
[15] B. Atasever, B. Ülküseven, T. Bal-Demirci, S. Erdem-Kuruca, Z. Solakoğlu, Invest New Drugs 28 (2010) 421.
[16] M. Hossain, S. Kumar Chattopadhyay, S. Ghosh, Polyhedron 19 (1997) 4313.
[17] S. Buscemi, M. Gruttadauria, Tetrahedron 56 (2000) 999.
[18] W.-K. Dong, J.-G. Duan, Y.-H. Guan, J.-Y. Shi, C.-Y. Zhao, Inorg. Chim. Acta 362 (2009) 1129.
[19] Bruker-AXS, APEX2/BIS, Madison, WI, 2010.
[20] G.M. Sheldrick, CELL-NOW, University of Göttingen, Germany, 2008.
[21] Bruker-AXS, SAINT, Madison, WI, 2009.
[22] G.M. Sheldrick, SADABS, University of Göttingen, Germany, 2008.
[23] G.M. Sheldrick, TWINABS, University of Göttingen, Germany, 2008.
[24] G.M. Sheldrick, Acta Crystallogr., Sect. A 64 (2008) 112.
[25] Bruker-AXS, SHELXTL, Madison, WI, 2008.
[26] A. El-Dissouky, M.M. Abou-Sekkina, M. El-Kersh, Z. El-Sonbati, Transition Met. Chem. 9 (1984) 372.
[27] V.K. Voronkova, J. Mrozinski, M.A. Yampol'skaya, Y.V. Yablokov, N.S. Evtushenko, M.S. Byrke, N.V. Gerbeleu, Inorg. Chim. Acta 238 (1995) 139.
[28] T. Bal Demirci, Y. Koseoglu, S. Guner, B. Ülküseven, Cent. Eur. J. Chem. 4 (2006) 149.
[29] W.-K. Dong, X.-N. He, H.-B. Yan, Z.-W. Lv, X. Chen, C.-Y. Zhao, X.-L. Tang, Polyhedron 28 (2009) 1419.
[30] V.M. Leovac, V. Divjakovic, V.I. Cesljevic, P. Engel, Polyhedron 6 (1987) 1901.
[31] M. Belicchi Ferrari, F. Bisceglie, G. Pelosi, P. Tarasconi, R. Albertini, S. Pinelli, J. Inorg. Biochem. 87 (2001) 137.
[32] M.A. Ali, A.H. Mirza, M.H.S.A. Hamid, P.V. Bernhardt, O. Atchade, X. Song, G. Eng, L. May, Polyhedron 27 (2008) 977.
[33] I.C. Mendes, L.M. Botion, A.V.M. Ferreira, E.E. Castellano, H. Beraldo, Inorg. Chim. Acta 362 (2009) 414.
[34] A. Böttcher, T. Takeuchi, K.I. Hardcastle, T.J. Meade, H.B. Gray, D. Cwikel, M. Kapon, Z. Dori, Inorg. Chem. 36 (1997) 2498.
[35] S. Di Bella, I. Fragalà, I. Ledoux, M.A. Diaz-Garcia, T.J. Marks, J. Am. Chem. Soc. 119 (1997) 9550.
[36] M. Şahin, T. Bal-Demirci, G. Pozan-Soylu, B. Üküseven, Inorg. Chim. Acta 362 (2009) 2407.
[37] N. Özdemir, M. Şahin, T. Bal-Demirci, B. Ülküseven, Polyhedron 30 (2011) 515.